IEEE Access
Multidisciplinary | Rapid Review | Open Access Journal

Received 3 February 2023, accepted 26 February 2023, date of publication 3 March 2023, date of current version 9 March 2023.

Digital Object Identifier 10.1109/ACCESS.2023.3252006

RESEARCH ARTICLE

Design of Bowtie Antenna With Rounded Edge and Middle-Sliced Modifications for UHF Partial Discharge Sensor

UMAR KHAYAM, (Member, IEEE), ASEP ANDI SURYANDI, AND RACHMAWATI
School of Electrical Engineering and Informatics, Institut Teknologi Bandung, Bandung 40132, Indonesia

Corresponding author: Umar Khayam (umar@itb.ac.id)

This work was supported by the World Class Research Program, Kemdikbudristek, Indonesia.

ABSTRACT Partial Discharge (PD) detection using ultra-high frequency (UHF) method has been proven as more noise-resistant in GIS condition monitoring, compared to the conventional PD detection methods, where the common noise frequency range such as in the power plants is below UHF frequency range. However, noise in UHF range may occur at certain conditions. Thus, UHF sensors with high sensitivity are necessary to detect PD-induced electromagnetic wave in UHF range. This paper discusses the modified design of a bowtie antenna as UHF sensor and its performance in detecting PD in the air. The modification method is conducted through simulation using antenna design software, resulting in rounded edge and middle-sliced bowtie antennas. The designed bowtie antenna has wider bandwidth of above 300 MHz, reflection coefficient lower than −10 dB, and the voltage standing wave ratio (VSWR) less than 2. During initial design, the antenna geometry including gap distance, wing radius, and flare angle are adjusted to obtain the optimum antenna characteristics. The final designed sensors are then fabricated on a printed circuit board (PCB) with FR4-epoxy substrate material and tested using Vector Network Analyzer (VNA). Furthermore, the modified antennas are also tested in the high voltage laboratory to detect PD in needle–plane electrode. The experiment results show that both modified bowtie antennas can successfully detect the PD signal with correct phase patterns, and that the middle-sliced modified bowtie antenna is more sensitive than the rounded-edge modified bowtie antenna.

INDEX TERMS Bowtie antenna, partial discharge, PD detector, UHF sensor.

I. INTRODUCTION

Gas Insulated Switchgear (GIS) has been widely existing in high voltage transmission systems for its benefits, such as compactness, simpler treatment, better dielectric performance, and high reliability. Nevertheless, the presence of metallic particles inside GIS may initiate partial discharge (PD) and lead to the breakdown in GIS. In order to monitor GIS condition and to detect any defect, the ultra-high frequency (UHF) method with a range of 300 MHz to 3 GHz, has been widely used to detect PD due to its sensitivity and resistance toward interferences [1], [2], [3]. With aim to increase reliability in power delivery, direct PD monitoring in HV equipment is indeed important as it can detect insulation failures immediately.

However, in GIS, PD detection using the very-high frequency (VHF), or low frequency (LF) method is not suitable for direct PD monitoring due to certain reasons, e.g., both VHF and LF methods are sensitive to external electrical disturbance, such as corona from the overhead lines. The induced corona amplitude is usually larger than PD which makes PD detection and characterization become difficult. Thus, in this case, PD detection using UHF is more suitable to monitor the equipment. This method has been widely used in HVAC tests, such as in IEC 62271-203. Due to the multipoint grounding system that is applicable completely in

The associate editor coordinating the review of this manuscript and approving it for publication was Pavlos I. Lazaridis.

TABLE 1. Types of Printable UHF Antennas for PD Detection [8], [9], [10], [11], [12].

Design	Size [mm^2]	Location	Application	Freq.range [GHz]
Planar monopole	340 x 140	External	Air insulated switchgear	0.34 – 8.0
Co-planar waveguide	282 x 242	—	—	0.4 – 3
Spiral	191 x 191	External	Electrical equipment	0.3 – 1.5
Log periodic	140 x 110	External		0.7 – 2.2
Fractal	126 x 108	Internal	Inverter-fed electrical machine	0.3 – 1.0
Microstrip	340 x 200	Internal	GIS	0.34 – 0.44
Vivaldi	100 x 100	Internal	—	1.3 – 3.0
Long Bowtie (LB)	125 x 53	External	GIS	0.81–2.63
Double Layer Bowtie (DLB)	85 x 43	External	GIS	1.5 – 2.07
Enhanced Bowtie antenna	74 x 36	External	GIS	1.27 – 2.49
Sliced Edge Bowtie (SEB)	76 x 18	External	GIS	1.33 – 1.78

GIS, PD detection using the UHF method is assumed as the most sensitive detection method these days, compared to the conventional method as in IEC 60270 [4], [5], [6], [7].

Most types of UHF antennas are large in dimension in order to improve gain and sensitivity for the purpose of early detection of PD [8]. Table 1 shows some types of printable UHF antennas with their dimension, application, and frequency range which are used for PD detection in medium and high voltage power apparatus. Certain applications, such as internal sensors in GIS require size reduction due to the limited space. Generally, the target of reduced antenna size while maintaining its performance with length below 200 mm to be installed on some dielectric windows [8], [9], [10], [11], [12]. However, as shown in Fig. 1, HV GIS with a lower voltage rate has a dielectric window of less than 100 mm in length, although it may have a larger size for GIS of higher voltage [13].

So far, the previously designed bowtie antennas, as shown in Table 1, have successfully reduced the size to be able to fit the smaller dielectric windows, although the frequency range may be more narrow compared to the other types of UHF antennas, and may result in smaller gain and sensitivity. In addition, among the printable UHF antennas, the bowtie antenna has the simplest structure, hence easier to fabricate and cost-effective. Alternatively, the gain problem can be solved by adding an amplifier to complement the work of the bowtie antennas.

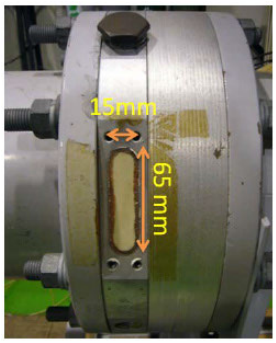

FIGURE 1. Spacer aperture of 66 kV GIS [13].

In our past research, there are many variations of UHF bowtie antenna modifications, such as enhanced bowtie antenna, sliced edge, modified long bowtie antenna, and double layer bowtie, as shown in Fig. 2 [9], [10], [11], [12]. Those modified bowtie antenna designs that are shown in Fig. 2 have characteristics with the comparison that are described in Table 2.

TABLE 2. Characteristic Comparison of Previous Modified Bowtie Antenna Designs.

Design	Reflection Coefficient (dB)	Bandwidth (MHz)
Enhanced Bowtie (EBT)	-16.8	245
Sliced Edge Bowtie (SEB)	-40.27	282
Long Bowtie (LB)	-17.43	202
Double Layer Bowtie (DLB)	-18.92	330

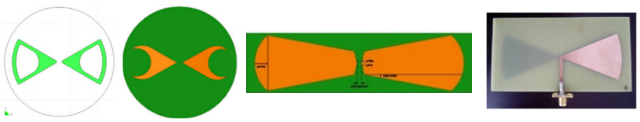

FIGURE 2. Modified bowtie antenna designs: (a) Enhanced bowtie (EBT), (b) Sliced-edge bowtie (SEB), (c) Long bowtie (LB), and (d) Double layer bowtie (DLB).

The objectives of this research are to design a UHF sensor in a form of a bowtie antenna which is used to detect and recognize PD in GIS with improved characteristics, such as the bandwidth, as well as to analyze the sensor's sensitivity in detecting PD sources. The sensor detects and captures electromagnetic (EM) waves radiated by PD sources [14], [15], [16], [17], [18], [19], [20]. These PD signals are then recorded in both frequency and time domains to obtain PD patterns and waveforms in each domain.

This paper elaborates on the design process of UHF bowtie antenna sensor for PD detection. For the initial design phase, it is important to determine the antenna's geometry including gap distance, wing radius, and flare angle to obtain optimum antenna characteristics. The antenna size should be

considered carefully as well to achieve a good performance as a PD detector.

These previously designed antennas still need to be further developed to obtain more optimized design with better antenna characteristics, which include the reflection coefficient that should be less than −10 dB, wider bandwidth (more than 330 MHz), and the voltage standing wave ratio (VSWR) value (less than 2). One of the methods to reduce the reflection coefficient is by distributing the current density more evenly across the surface of an antenna. Therefore, the new modifications of the bowtie antenna discussed in this paper are started from the investigation of the current density distribution of a regular bowtie antenna itself. The idea of the new modification of the bowtie antenna is to eliminate the parts of the antenna where the current distribution is not uniform.

The new modifications of the bowtie antenna that are differed from the previous ones consist of two types of modifications, which are the rounded edge of the antenna and the middle-sliced of the antenna wings. Several steps are performed in the design process of the newly modified bowtie antenna, starting from the optimization of the bowtie antenna's basic characteristics and the modification itself that are conducted through design and simulation software. The optimum designs of the modified bowtie antennas are then fabricated on a PCB with FR4-epoxy substrate material and the antenna characteristics are verified using Vector Network Analyzer (VNA). Although the ultimate goal of these UHF antennas is for PD detection in GIS, however at this stage, the purpose is to ensure that the modified bowtie antennas are able to detect and measure PD signals, hence PD detection test in the air is conducted in HV laboratory using a needle-plane electrode as PD source.

II. DESIGN AND SIMULATION

A. INITIAL DESIGN OF BOWTIE ANTENNA

In this research, the designed UHF antenna will be utilized for PD detection in GIS. The frequency spectrum of PD-induced electromagnetic waves in GIS is in the range of 300 MHz to 3 GHz. Thus, bowtie antennas which are able to detect PD in that frequency range are designed with increased bandwidth compared to the previously designed bowtie antennas. The design criteria of the antenna characteristics are a reflection coefficient of less than −10 dB, wider bandwidth (more than 330 MHz) within the frequency range of 300 MHz – 3 GHz, and voltage standing wave ratio (VSWR) of less than 2.

Prior to designing a modification of a bowtie antenna, the initial design itself requires some optimizations on its dimensions to obtain optimum initial antenna characteristics. This stage of the process is conducted through an antenna design software that uses the Finite Element Method (FEM) simulation method in 3D, where an image of a designed antenna in a form of a 2-dimensional (2D) perfect electric boundary is placed on an XY plane surrounded by air boundary with relative permittivity of 1 and at a distance of 250 mm. The adjusted initial antenna dimensions that include wing radius, flare angle, and gap distance are expected to have effects on frequency response characteristics. Modifications on the antenna geometry parameters affect the current distribution on the antenna surface. An antenna with evenly distributed surface current density is preferable since it can improve the efficiency of the antenna. The antenna's efficiency can be quantified by measuring the reflection coefficient. In addition, a lower reflection coefficient would result in wider bandwidth. Therefore, in the initial design step, the variations in antenna geometry parameters are simulated and determined by evaluating the reflection coefficient graph as well as the resulting bandwidth.

1) WING RADIUS

There are four types of wing radius, which are 10 mm, 20 mm, 30 mm, and 40 mm that results in different reflection coefficient graphs, as shown in Fig. 3. The simulation result shows the different resonant frequency for each model where the larger wing radius results in smaller resonant frequency. The effect of changed wing radius on resonant frequency is caused by the signal wavelength, whereas at a higher frequency, the wavelength is shorter. Based on the graph, the antennas with wing radius of 10 mm and 30 mm have similarly lower reflection coefficients (∼−21.5 dB) compared to those of 20 and 40 mm wing radius, with the resonant frequency of 1.4 and 3.4 GHz, respectively. However, based on previous research, PD signal often occurs at the frequency range of

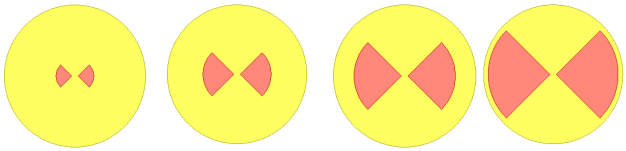

(i) r = 10 mm (ii) r = 20 mm (iii) r = 30 mm (iv) r = 40 mm

(a) Variations on wing radius

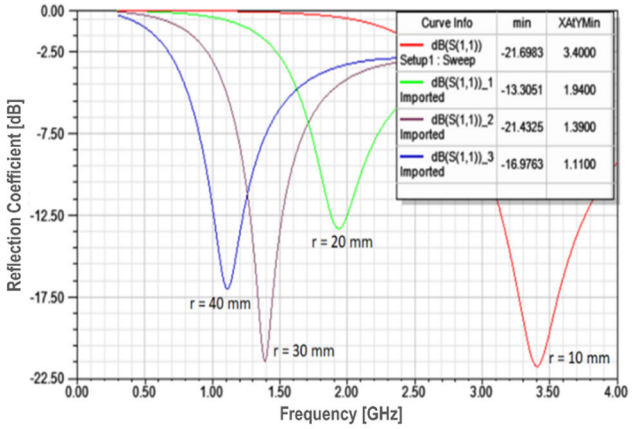

(b) Reflection coefficient graph of varied wing radius

FIGURE 3. Reflection coefficient characteristics of varied wing radius of a bowtie antenna.

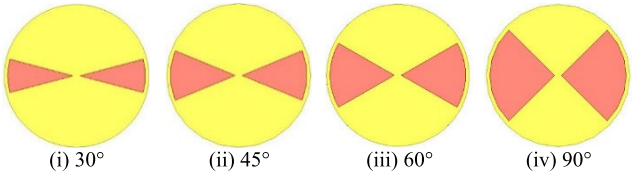

(a) Variations on flare angle

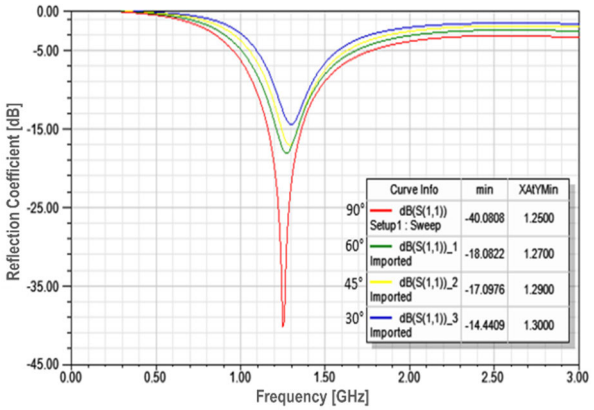

(b) Reflection coefficient graph of varied flare angle

FIGURE 4. Reflection coefficient characteristics of varied flare angles of a bowtie antenna.

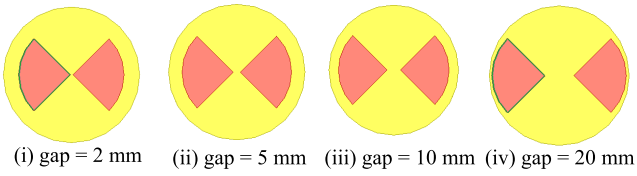

(a) Variations in gap distance

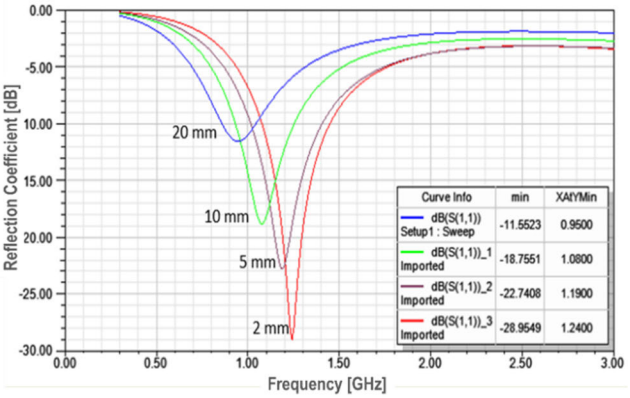

(b) Reflection coefficient graph of varied gap distance

FIGURE 5. Reflection coefficient characteristics of varied gap distance of a bowtie antenna.

below 1 GHz. Thus, the antenna with a 30 mm wing radius with a resonant frequency is 1.4 GHz is chosen in this design.

2) FLARE ANGLE

Four variations on flare angle of the bowtie antenna consists of 30°, 45°, 60°, and 90° flare angle. The illustration of these varied flare angles and the simulation results on the reflection coefficient graph is shown in Fig. 4. Based on the result, it shows that the reflection coefficient as well as the resonant frequency decreases along with an increase of the flare angle. The change in flare angle affects the reflection coefficient for the resulting resonant frequency of the antenna. Thus, the chosen design is the bowtie antenna with a 90° flare angle since it has the lowest reflection coefficient of −40.08 dB.

3) GAP DISTANCE

Gap distance refers to the distance that separates the innermost points of each bowtie arm. The variation on this parameter consists of 2 mm, 5 mm, 10 mm, and 20 mm gap distances, as shown in Fig. 5, along with the simulation result of the reflection coefficient. The graph shows that a smaller gap distance resulted in a lower reflection coefficient but higher resonant frequency. From this result, it is determined that the gap distance for the initial antenna design is 2 mm which results in the smallest reflection coefficient of −28.96 dB.

These previously determined initial bowtie antenna dimensions, which are 30 mm wing radius, 90° flare angle and 2 mm gap distance resulted in the optimum frequency response of a bowtie antenna, as shown in Fig. 6. The optimum antenna characteristics that are obtained by this initial design include the low resonance frequency of 1.24 GHz, which is the closest

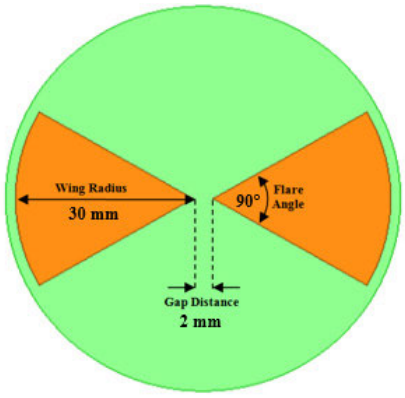

(a) Initial design dimension

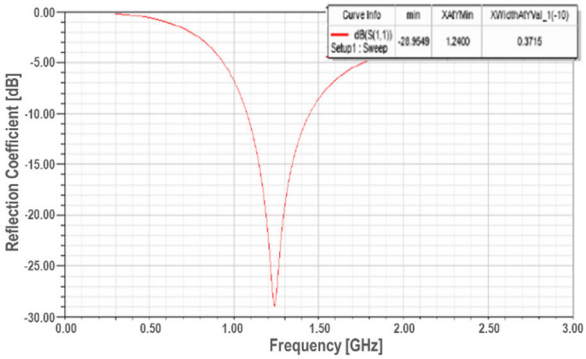

(b) Reflection coefficient characteristics of initial design of bowtie antenna

FIGURE 6. Initial design of bowtie antenna and its responding reflection coefficient characteristics.

to PD signal frequency range, the lowest reflection coefficient of -28.96 dB, and bandwidth of 371 MHz.

In addition to the determined dimensions above, the material specifications, such as type of material, thickness and diameter are also determined in this stage based on the resulting optimum characteristics. The chosen substrate material is PCB material, which is FR4-epoxy ($\varepsilon_r = 4.4$) with a thickness of 1.6 mm and shaped as a circle with a diameter of 90 mm. This substrate material and the thickness are determined by the resulting lower frequency response (closer to PD signal frequency range) and lower reflection coefficient.

The current density distribution of the bowtie antenna with the determined parameters is investigated afterward. An antenna has different impedances at every single point on the antenna surface which causes the current density to be distributed unequally throughout the antenna surface. In order to determine the part that should be eliminated due to uneven density distribution, Fig. 7 shows the current density distribution of the initial bowtie antenna, which is uniform from the innermost up to the middle of the antenna, except on the edge of the antennas where current density decreases. Therefore, the antenna is modified by cutting the edge of the antennas with circular shape, and by cutting the middle part to result in more uniformly distributed current density.

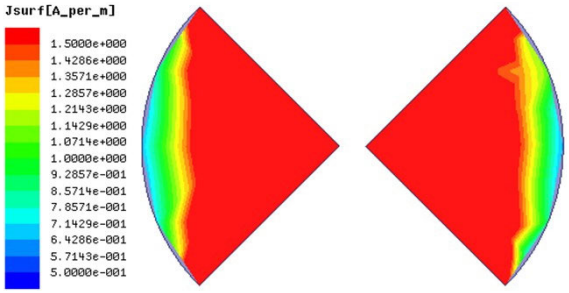

FIGURE 7. Current density distribution of an original bowtie antenna.

B. MODIFICATIONS ON BOWTIE ANTENNA

1) ROUNDED EDGE MODIFICATION

The first modification to the bowtie antenna is the rounded edge of the antenna wings with various edge radius (r_e), as shown in Fig. 8. Based on the previous research, the change of the edge shape has been proven to give lower reflection coefficient of an antenna [21], [22], [23], [24]. Then, the simulation on this parameter is performed to obtain the optimum shape.

The variation on r_e give antenna characteristic result as shown in Fig. 9.

The simulation results have shown that r_e of 20 mm gives the lowest reflection coefficient of −24.49 dB at the resonance frequency of 1.59 GHz. Due to this modification, the initial antenna surface area of 1,412 mm^2 is reduced to 1,041 mm^2.

Next, to ensure that this design has fulfilled the desired characteristics of evenly distributed current distribution, the current distribution is also evaluated on the rounded edge bowtie antenna with various r_e, as shown in Fig.10. It is

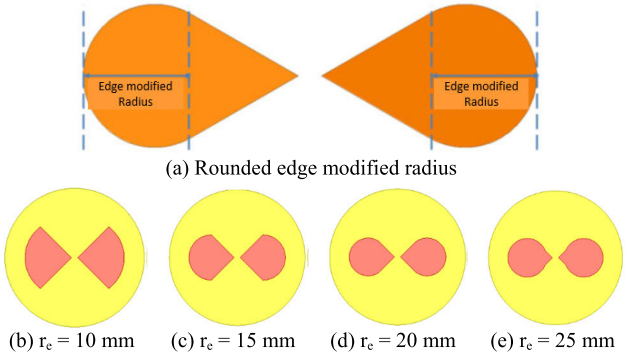

FIGURE 8. Variations in radius of rounded edge modification.

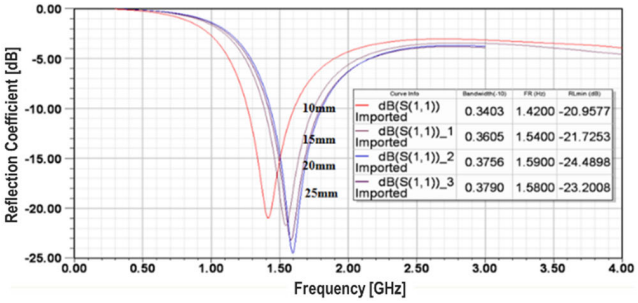

FIGURE 9. Reflection coefficient characteristics of varied rounded edge radius of modified bowtie antenna.

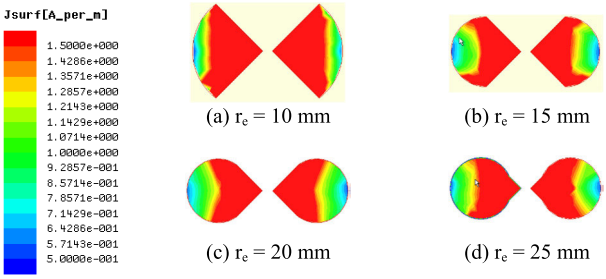

FIGURE 10. Rounded edge modified bowtie antenna with various r_e.

expected that analysis of the current distribution of an antenna can be used to reduce its reflection coefficient.

It can be seen from the figure that the outermost of the antenna has the lowest current density. In addition, the rounded shape of the antenna edges indeed gives more evenly distributed current density to the middle part of the antenna (Figs. 10(c) and (d)), compared to the initial design of the bowtie antenna where the higher current density is only spotted on the edge corner of the antenna in Fig. 7. By combining the analysis results on current density distribution and the reflection coefficient characteristics results of various r_e, it is determined that the selected radius for rounded edge bowtie antenna is 20 mm.

The final design of the rounded edge modified bowtie antenna with a gap distance of 2 mm, flare angle of 90°, wing

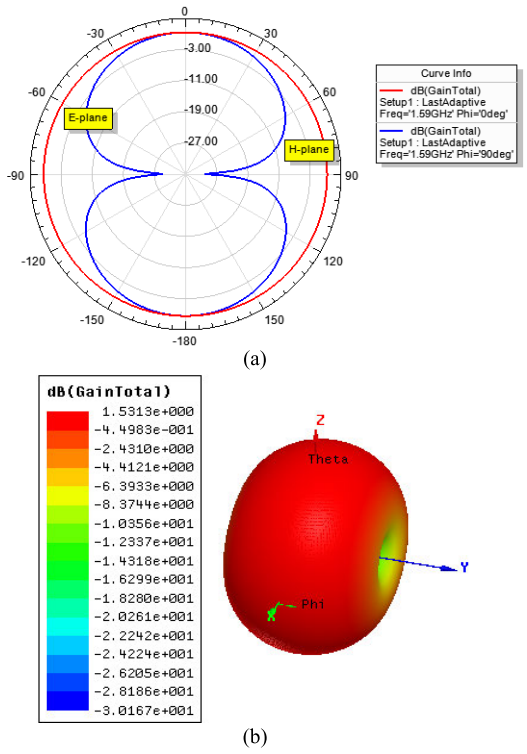

FIGURE 11. (a) 2D and (b) 3D radiation pattern of rounded edge modified bowtie antenna at the resonant frequency of 1.59 GHz.

radius of 30 mm, and r_e of 20 mm has a radiation pattern, as shown in Fig. 11.

According to Fig. 11 (a), the rounded edge modified bowtie antenna has omnidirectional radiation characteristic in H-plane, and dipole-like characteristic of E-plane. These characteristics are desirable for antennas designed for PD detection in power substations, since they can detect PD signals from all directions. In Fig. 11 (b), the optimal design of rounded edge modified bowtie antenna has gain of 1.53 dB at its resonant frequency of 1.59 GHz.

2) MIDDLE-SLICED MODIFICATION

Another modification that is applied to this bowtie antenna after the first modification is slicing the middle part of antenna wings with the aim to get more uniform current density. In this modification process, the current density distribution is once again monitored, as shown in Fig. 12. The figure shows that this modification has resulted in more uniformly distributed current density throughout the antenna.

The varying parameter that is performed on this middle-sliced modification is the ratio between the sliced part and the full-scale size of the antenna, which is shown in equation (1) below.

$$\text{Slicing scale} = \frac{\text{Sliced partsurface area}}{\text{Initial surface area}} \tag{1}$$

The slicing scale of this modification is changed from 0.6 to 0.9, as shown in Fig. 13. Meanwhile, the form of the antenna wings remains identical to the first modified design.

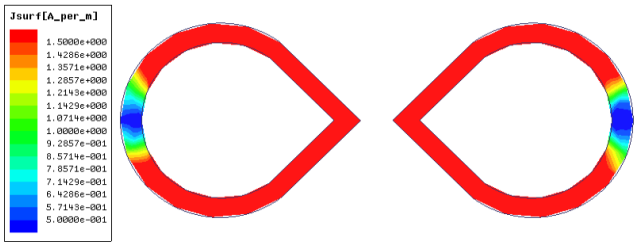

FIGURE 12. Current density distribution of middle-sliced modified bowtie antenna.

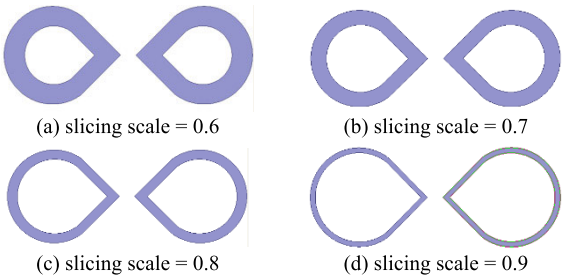

FIGURE 13. Middle-sliced modification on the bowtie antenna with various slicing scales.

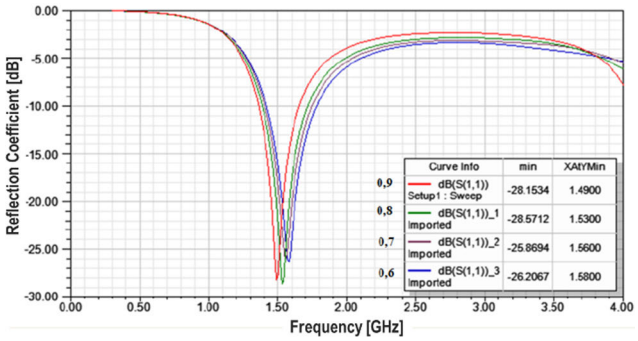

FIGURE 14. Reflection coefficient characteristics of varied slicing scale of middle-sliced modified bow tie antenna.

The simulation results of this modification are shown in Fig. 14 where the lowest reflection coefficient is achieved by the middle-sliced modified bowtie antenna with a slicing scale of 0.8, resulting in the most optimum reflection coefficient of −28.57 dB at the resonant frequency of 1.53 GHz. As for the other ratios of 0.6, 0.7, and 0.9 slicing scale, the reflection coefficients are −26.21 dB, −25.87 dB, and −28.15 dB at the resonant frequency of 1.58 GHz, 1.56 GHz, and 1.49 GHz respectively.

The final design of a middle-sliced modified bowtie antenna consisting of gap distance of 2 mm, flare angle of 90°, wing radius of 30 mm, rounded edge modified radius of 20 mm, and slicing scale of 0.8, has radiation pattern as shown in Fig. 15, which is measured at the resonance frequency of 1.53 GHz. Similar to the rounded edge modified bowtie antenna, the H-plane is also omnidirectional, while the E-plane has dipole characteristic. Thus, in terms of the radiation pattern, both the rounded edge and the middle-sliced

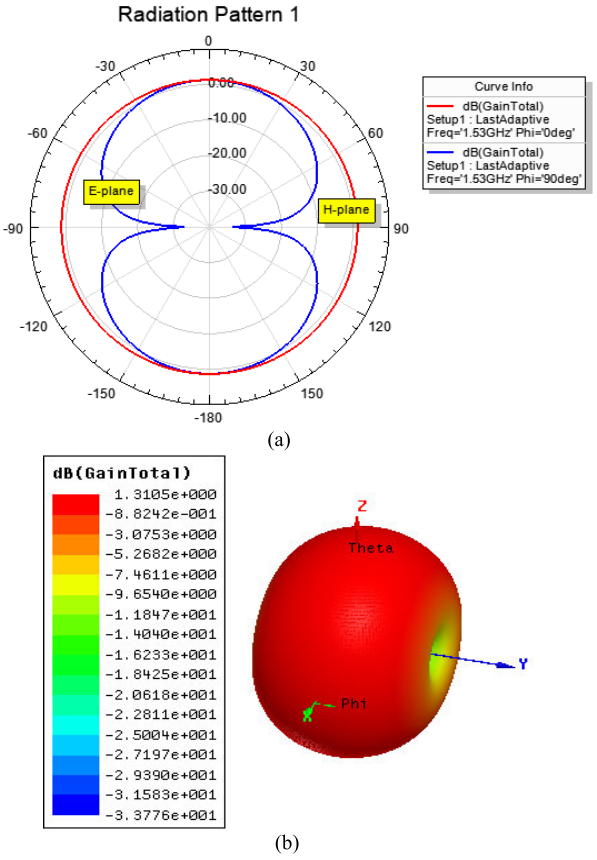

FIGURE 15. (a) 2D and (b) 3D radiation pattern of middle-sliced modified bow tie antenna at the resonant frequency of 1.53 GHz.

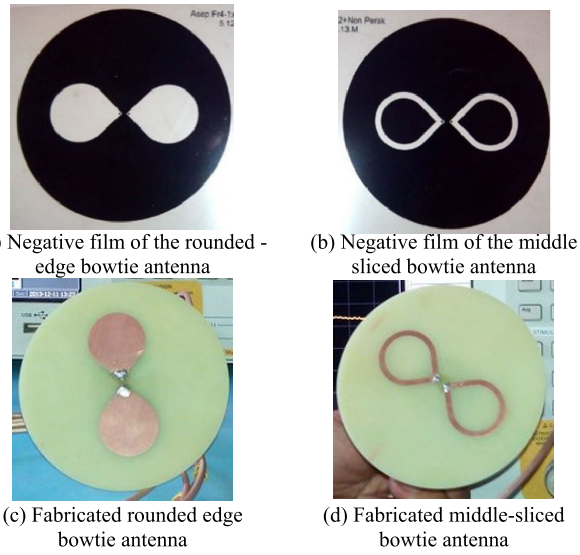

FIGURE 16. Fabricated modified bowtie antenna.

modified bowtie antennas are suitable as UHF antennas for detecting PD in all directions.

The 3D radiation pattern in Fig. 15 (b) shows that the gain of the middle-sliced modified bowtie antenna is 1.31 dB at its resonance frequency of 1.53 GHz, which is lower than that of the rounded edge modified bowtie antenna. According to these results, the rounded edge modified bowtie antenna is expected to have higher gain during PD measurement compared to the middle-sliced modified bowtie antenna.

C. ANTENNA FABRICATION

The final design of the antenna is then fabricated on a PCB material with FR4-Epoxy substrate with permittivity (ε_r) of 4.4 and thickness of 1.6 mm, by using a photo image transfer method with accuracy is up to 0.254 mm. Dry Film Photoresist (Photo Sensitive Film) is used as the material where the negative film is required as the artwork (for image transfer). The negative film of the designed antenna and the fabricated modified bowtie antenna is shown in Fig. 16.

III. ANTENNA TESTS

Two types of tests are performed to the fabricated of new modified bowtie antennas, which are antenna characteristic measurement using a Visual Network Analyzer (VNA) and PD detection to examine the ability of the designed antennas in detecting PD in the air from a PD source.

A. ANTENNA CHARACTERISTICS MEASUREMENT USING VNA

In order to observe the antenna characteristics of these new modified bowtie antennas, both antennas are first tested using VNA at a UHF frequency range of 300 MHz to 3 GHz, where there are 201 measurement points with an interval of 15 MHz. The measured parameters are the bandwidth, reflection coefficient and the corresponding resonant frequency, as well as VSWR. The reflection coefficient measurement results and the comparison to those obtained from the simulations are shown in Fig. 17.

Based on the figure, the reflection coefficient measurement result of the rounded edge bowtie antenna shows just a slight difference from the simulated one as, shown in Fig. 17(a), where the measured reflection coefficient is −21.795 dB at the resonant frequency of 1.56 GHz and the simulated reflection coefficient is −24.49 dB at the resonant frequency of 1.59 GHz. As for the middle-sliced bowtie antenna, the measured reflection coefficient is rather different from the simulation result, where the measured reflection coefficient is −23.218 dB at the resonant frequency of 1.395 GHz and the simulated reflection coefficient is −28.571 dB at the resonant frequency of 1.53 GHz, showing 5.35 dB-gap between the measured and simulated reflection coefficient values. It could happen due to concrete environmental conditions during experiments, such as the presence of additional adapters and connectors, limitations on the used software as well as in the final fabrication.

From Fig. 17, the bandwidth of the rounded edge bowtie antenna for a reflection coefficient lower than −10 dB is 450 MHz with a frequency range of 1.41–1.86 GHz. Meanwhile, in the simulation for a reflection coefficient lower than

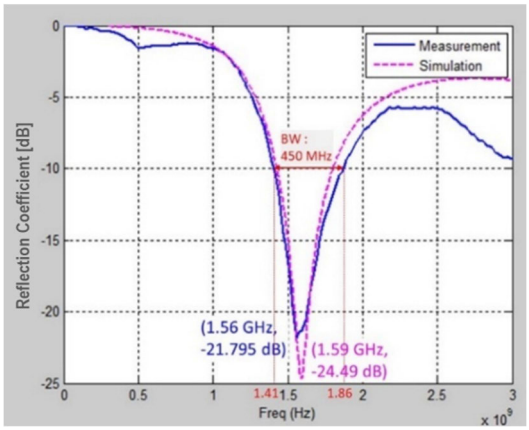

(a) Reflection coefficient of rounded edge bowtie antenna

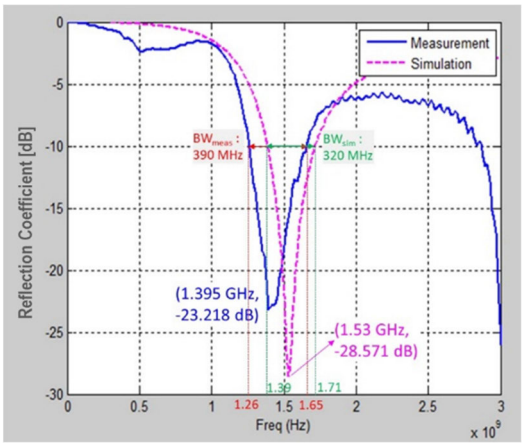

(b) Reflection coefficient of middle-sliced bowtie antenna

FIGURE 17. Reflection coefficient characteristics comparison between the VNA measurement and the simulation results.

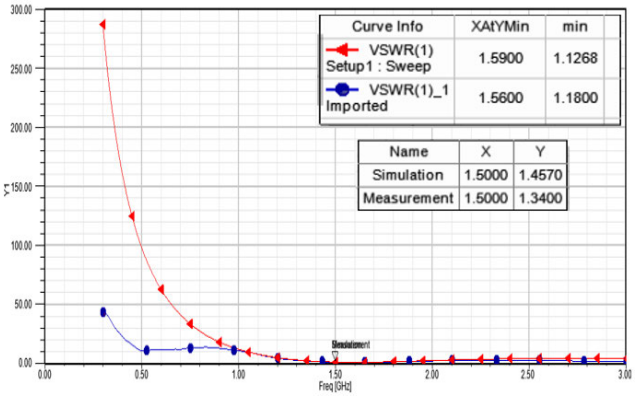

(a) VSWR of the rounded edge bowtie antenna

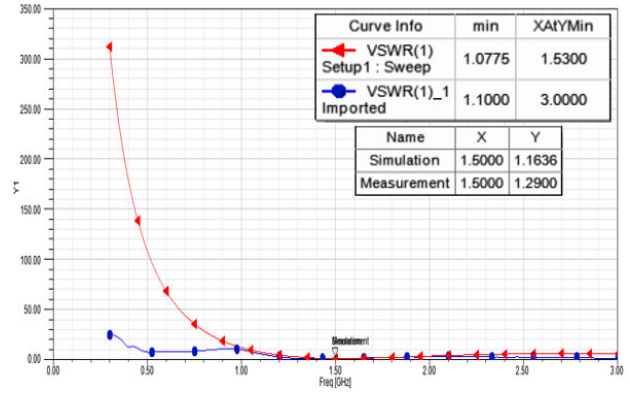

(b) VSWR of the middle sliced bowtie antenna

FIGURE 18. VSWR comparison between VNA measurement and simulation results.

−10 dB, the bandwidth is 376 MHz with a frequency range of 1.43–1.80 GHz. The bandwidth measurement results of the middle-sliced bowtie antenna are 390 MHz with a frequency range of 1.26–1.65 GHz. Meanwhile, the antenna bandwidth of the simulation results is 320 MHz with a frequency range of 1.39–1.71 GHz.

The next measured parameter is the VSWR of both types of modified bowtie antennas, which are shown in Fig. 18. The graph shows that the rounded edge bowtie antenna has both measured and simulated VSWR values of less than or equal 2 (VSWR $\leq$ 2) at the frequency of 1.5 GHz, where the measured and the simulated VSWR values are 1.34 and 1.457, respectively. For the middle-sliced bowtie antenna (Fig. 18(b)), both measurement and simulation results show that VSWR is less than or equal 2 (VSWR $\leq$ 2) at the frequency of 1.5 GHz, where the measured and the simulated VSWR values are 1.29 and 1.1636, respectively.

The last measured parameter is antenna resistance through Smith Chart, as shown in Fig. 19. The graph shows that at its resonance frequency, the resistance value is approximately 50 Ω, although there is still some reactance that affects the antenna quality in detecting signal.

TABLE 3. Antenna Characteristics Test Results Comparison Using VNA and Simulation.

Antenna Characteristics	Initial Shape	Rounded-edge Modified Bowtie Antenna	
		Measurement	Simulation
1. Bandwidth [MHz]	371	450	376
2. Reflection Coefficient [dB]	-28.96	-21.795	-24.49
3. VSWR	< 2	1.34 (≤ 2)	1.46 (≤ 2)
4. Area [mm^2]	1412	1041	
		Middle-sliced Modified Bowtie Antenna	
1. Bandwidth [MHz]		390	320
2. Reflection Coefficient [dB]		-23.218	-28.571
3. VSWR		1.29 (≤ 2)	1.16 (≤ 2)
4. Area [mm^2]		375.1	

In summary, the characteristics test results of both new modified bowtie antennas using VNA are shown in Table 3.

Overall, the antenna test results using VNA show relatively similar results as expected from the simulation results. The differences that occur between the measurement and the simulation result can be caused by imperfect antenna fabrication and the presence of additional adaptors or connectors. It also

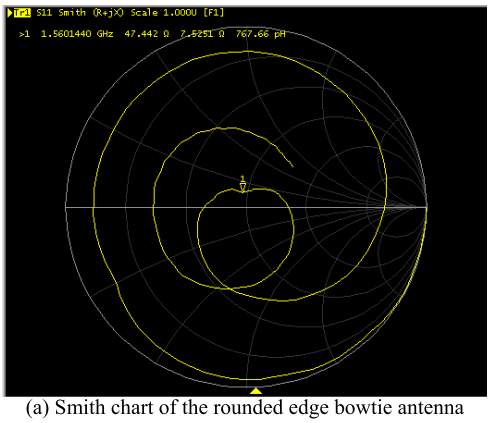

(a) Smith chart of the rounded edge bowtie antenna

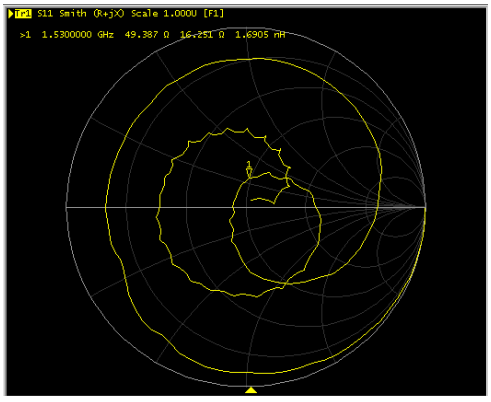

(b) Smith chart of the middle-sliced bowtie antenna

FIGURE 19. Smith chart (antenna resistance) of the modified bowtie antennas.

can be caused by a limitation in computation during simulation which may result in inaccuracy.

B. PD DETECTION TESTS

To investigate the antennas capability in detecting PD, PD detection experiments are conducted in the air with the experimental set-up and the actual set-up image in the laboratory as shown in Fig. 20 and Fig. 21, respectively.

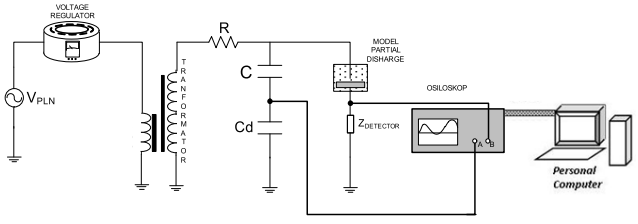

FIGURE 20. PD detection experimental set up.

The PD source that is used in this test is a needle-plane electrode with a gap of 10 mm. There are two sensors that are used in detecting PD, which are the antenna itself and the RC detector as a comparison. The distance between the PD source and the antenna is set to 100 mm first and then increased to 200 mm and 300 mm to check the performance of each antenna with varied distances.

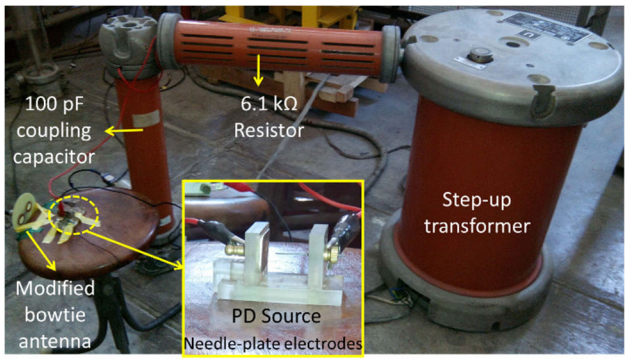

FIGURE 21. PD detection experimental set up in the laboratory.

TABLE 4. PDIV(-) Comparison of Both Modified Bowtie Antennas at Distance of 100 mm.

PD Parameters	Rounded edge modified bowtie antenna	Middle-sliced modified bowtie antenna
PDIV [kV source]	3.5	3.4
V_{pp} [mV]	29	34
Rise time [ns]	2	2
Fall time [ns]	4	3

During the measurement, parameters, such as PDIV, PD magnitude at certain voltage levels, and (φ-q-n) pattern are measured. Table 4 shows the negative PDIV measurement results of both modified bowtie antennas at a distance (d) of 100 mm.

Table 4 shows that inception PD is detected earlier by the middle-sliced modified bowtie antenna than the rounded edge modified bowtie antenna. The measured PD magnitude at each PDIV is also larger for the middle sliced modified bowtie antenna than that of the rounded edge modified bowtie antenna. This result shows that the middle-sliced modified bowtie antenna is more sensitive than the rounded edge modified bowtie antenna.

To see if this result is consistent with increasing distance, Fig. 22 shows the PDIV of both modified bowtie antennas at various distances. In the figure, both negative and positive PDIV of the middle-sliced modified bowtie antenna are almost always lower than those of the rounded edge modified bowtie antenna at each varying distance. It shows that the middle-sliced modified bowtie antenna is more sensitive than the rounded edge one, except for positive PDIV at d = 300 mm where PDIV of the middle-sliced modified bowtie antenna is higher than that of the rounded edge modified bowtie antenna.

Fig. 23 shows the rise time (t_{rise}) and fall time (t_{fall}) of each PD signal detected by both modified bowtie antennas at PDIV and voltage levels higher than PDIV by 1.5 or 2 times. It is clear that for most PD signals at each similar voltage level, t_{rise} and t_{fall} of those detected by the middle-sliced modified bowtie antenna are much lower than those of the rounded edge modified bowtie antenna. It implies that the

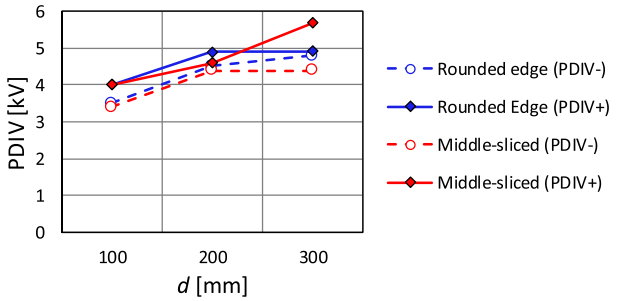

FIGURE 22. PDIV at various distances between antenna and PD source.

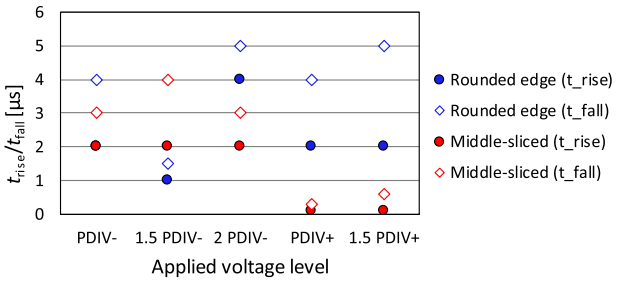

FIGURE 23. t_{rise} and t_{fall} of PD signals detected by modified bowtie antenna at various voltage levels.

TABLE 5. PDIV Measurement Results at Distance of 200 mm.

Applied voltage level	Rounded edge	RC detector	% V_{RE}/V_{RC}	Middle-sliced	RC detector	% V_{MS}/V_{RC}
Negative PDIV						
PDIV	60	95	63%	20	106	19%
5.2 kV	60	102	59%	18	114	16%
6 kV	-	-	-	21	120	17%
Positive PDIV						
PDIV	-	-	-	25	360	7%
5.2 kV	50	80	63%	36	850	4%
6 kV	100	160	63%	36	900	4%

middle-sliced modified bowtie antenna is more sensitive to detect PDs with shorter pulse sequences.

Fig. 24 shows PD waveforms at various voltage levels and at $d = 100$ mm. The comparison of PDIV and PD signals magnitude can be seen in Fig. 25. At $d = 100$ mm, the magnitude of PD signals detected by the middle-sliced modified bowtie antennas are larger than or equal to those of the rounded edge modified bowtie antenna.

PD measurement results at d = 200 mm and 300 mm are presented in Table 5 and Table 6, respectively, where PD magnitude detected by the rounded edge and the middle-sliced bowtie antennas in comparison with each of their respective RC detector measurement results can be observed. The percentage in the table shows the ratio between PD magnitude of the bowtie antennas and its respective PD magnitude of the RC detector.

Based on Tables 5 and 6, for the same PD type, the same applied voltage level, and the same distance to the PD source, PD signals detected by the rounded edge bowtie

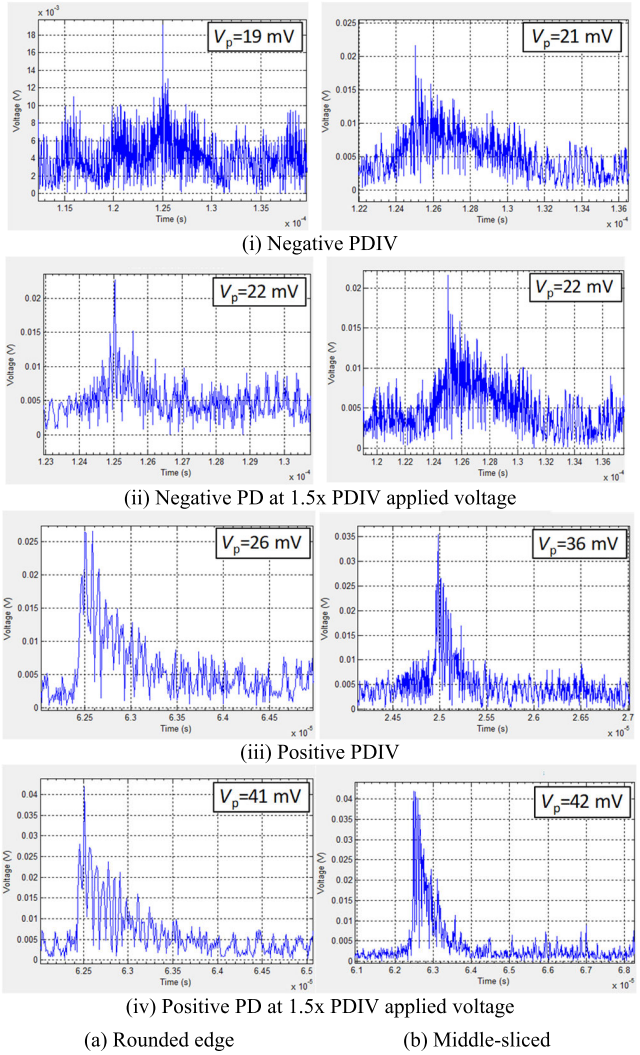

FIGURE 24. PDIV and PD signals waveforms detected by (a) the rounded edge and (b) middle-sliced bowtie antennas at the same voltage levels at d = 100 mm.

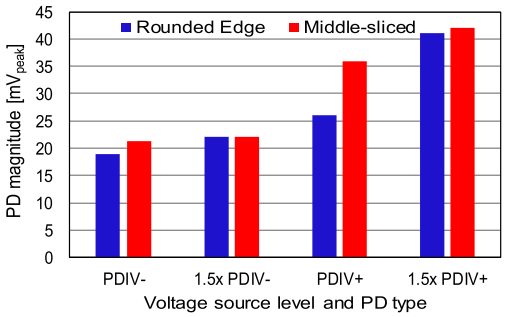

FIGURE 25. Comparison of PD magnitude measured by the rounded edge and the middle-sliced bowtie antennas at d = 100 mm.

antenna are larger than those of the middle-sliced bowtie antenna in terms of magnitude as well as the ratio with each respective RC detector measurement results. However, as distance increases, the PD magnitude measured by the rounded edge bowtie antenna decreases more than

TABLE 6. PDIV Measurement Results at Distance of 300 mm.

Applied voltage level	Rounded edge	RC detector	% V_{RE}/V_{RC}	Middle-sliced	RC detector	% V_{MS}/V_{RC}
Negative PDIV						
PDIV	41	95	43%	21	160	13%
5.2 kV	50	110	45%	24	164	15%
6 kV	45	95	47%	30	204	15%
Positive PDIV						
PDIV	34	500	7%	23	450	5%
5.2 kV	39	600	7%	58	1400	4%
6 kV	45	710	6%	60	3000	2%

those of the middle-sliced bowtie antenna. It shows that the middle-sliced bowtie antenna may be more sensitive than the rounded edge modified bowtie antenna, where the middle-sliced bowtie antenna has always been able to detect PD signals at each different voltage and distance, but the rounded edge bowtie antenna measured PD signals closer to the RC detector measurement results, especially at a shorter distance to PD source.

The last parameter measured in the PD detection test is (φ-q-n) pattern. The obtained data of (φ-q-n) pattern are 125 cycles for each antenna at 3 types of voltage levels, which are 4 kV, 5.2 kV, and 6 kV. The measurement results of (φ-q-n) patterns are shown in Table 7.

PD signal occurs for the first time during the negative half cycle and more of them occur as the source voltage increases. At higher voltage levels, PD starts to occur during the positive half cycle. This phenomenon can happen because the process of initial electrons emitted from the needle tip of the electrode which can initiate negative discharges is much easier than the process of initial charge during the negative half-cycle period to initiate positive discharges unless more energy in the form of the source voltage is increased. This phenomenon also happens in this PD measurement experiment using these modified bowtie antennas, i.e., both antennas worked properly in detecting PD in air resulting from the PD source of the needle-plane electrode.

IV. DISCUSSIONS

Through PD detection tests, the rounded edge and middle-sliced modified bowtie antennas are proven to have worked properly in detecting PD in the air. In order to compare whether these new modified bowtie antennas have better antenna characteristics than the bowtie antennas in the previous research, Table 8 shows the comparison of antenna characteristics of all types of bowtie antennas.

Table 8 shows that the current modified bowtie antennas in the form of rounded edge and middle-sliced have better antenna characteristics, including lower reflection coefficient and wider bandwidth compared to the modified bowtie antennas from the previous research. These results also imply that both modified antennas are able to detect and measure PD in a wider frequency range within the UHF range and with higher efficiency. Based on the antenna characteristics, the middle-sliced modified bowtie antenna has higher efficiency than the rounded edge modified bowtie antenna.

The performance comparison of both modified bowtie antennas can be identified by PD measurement results. PDIV measurement results show that the middle-sliced modified bowtie antenna detects PD earlier than the other type. The rise time and the fall time of PD signals detected by the middle-sliced modified bowtie antenna are also shorter than those of the rounded edge modified bowtie antenna. This result indicates that the middle-sliced bowtie antenna is more sensitive than the rounded edge modified bowtie antenna in detecting PD with a shorter pulse sequence. PD measurement

TABLE 7. PD (φ-q-n) Pattern Measurement Results Detected by Modified Bowtie Antennas.

Voltage [kV]	Rounded edge bowtie antenna		Middle-sliced bowtie antenna	
4	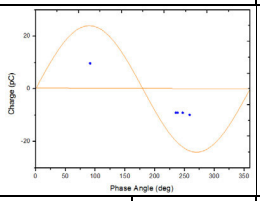		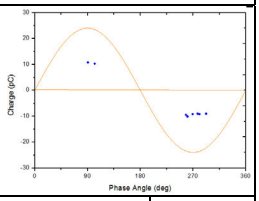	
PD type	PD-	PD+	PD-	PD+
φ	38.16	2.16	45.36	24.48
n	8	2	14	5
5.2	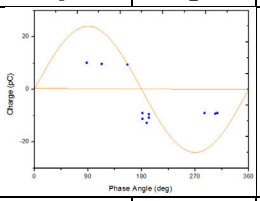		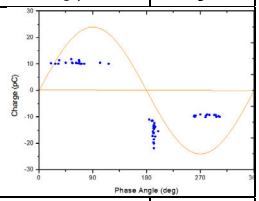	
PD type	PD-	PD+	PD-	PD+
φ	126	87.12	118.08	96.48
n	25	11	35	20
6	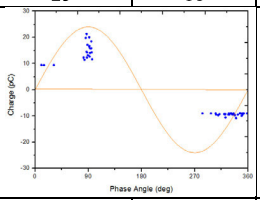		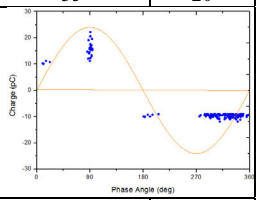	
PD type	PD-	PD+	PD-	PD+
φ	75.62	85.68	178.66	84.24
n	32	22	120	28

TABLE 8. Comparison of Antenna Characteristics between New and Previously Modified Bowtie Antennas.

Antenna Designs	Reflection Coefficient [dB]	Bandwidth [MHz]
Previous research:		
Enhanced Bowtie (EBT)	-16.8	245
Sliced edge Bowtie (SEB)	-40.27	282
Long Bowtie (LB)	-17.43	202
Double Layer Bowtie (DLB)	-18.92	330
Current research:		
Rounded edge Bowtie	-21.795	450
Middle sliced Bowtie	-23.218	390

TABLE 9. The Effects of Bowtie Antenna Parameters on Frequency Response Characteristics.

Bowtie antenna parameters	Effects on Frequency Response Characteristics		
	Resonant frequency	Bandwidth	Minimum reflection coefficient
Wing radius	inverse proportional	-	-
Flare angle	-	inverse proportional	inverse proportional
Gap distance	-	inverse proportional	proportional

results with varying distance show that the middle-sliced modified bowtie antenna always detects negative and positive PD at any applied voltage and at any distance from 100 to 300 mm, showing higher sensitivity compared to the rounded edge modified bowtie antenna. The same conclusion can also be obtained by (φ-q-n) pattern measurement results, where at each of the same voltage source levels, the number of PD detected by the middle-sliced modified bowtie antenna is always more than by the rounded edge modified bowtie antenna. Therefore, the middle-sliced modified bowtie antenna is considered to have higher sensitivity than the rounded edge modified bowtie antenna. It is also in accordance with the measured antenna characteristic by VNA which shows that the middle-sliced modified bowtie antenna has higher efficiency than the rounded edge modified bowtie antenna.

On the other hand, PD measurement results at various distance show that the magnitude of PD signals at $d =$ 200 mm and $d = 300$ mm which are detected by the rounded edge modified bowtie antenna are larger up to three times than those of the middle-sliced modified bowtie antenna. This result proves that the rounded edge modified bowtie antenna has a higher gain than the middle-sliced modified bowtie antenna. This result is in accordance with the radiation pattern simulation results that show the rounded edge modified bowtie antenna has a higher gain (1.53 dB) than the middle-sliced modified bowtie antenna (1.31 dB).

From the design process, the effect of changing dimension of an antenna can also be learned. The change of wing radius affects the resonant frequency of an antenna, i.e., a larger wing radius results in a smaller resonant frequency. It is caused by the signal wavelength, where at a higher frequency, the wavelength is shorter. The flare angle has an effect on the reflection coefficient value as well as the resonant frequency, where these parameters decrease along with the increase of the flare angle. The last dimension parameter that has effect on antenna characteristics is the gap distance between the innermost points of antenna arms, where a smaller gap distance results in a lower reflection coefficient value, but higher resonant frequency. The effects of change in bowtie antenna dimension parameters on frequency response characteristics of the antenna are also summarized in Table 9.

Eventually, in designing a bowtie antenna, many dimension parameters of the bowtie antenna can be adjusted with those rules to acquire more specific antenna characteristics.

V. CONCLUSION

The new modifications on bowtie antennas which consist of rounded edge and middle-sliced modifications are conducted first by observing the current density distribution throughout the antenna surface and determining the shape that has the optimum characteristic result through simulation using the FEM method. Both modified antennas are then fabricated on an FR4-epoxy substrate material and tested using VNA, showing that the rounded edge modified bowtie antenna has reflection coefficient of -21.795 dB, bandwidth of 450 MHz, and VSWR of 1.34, while the middle-sliced modified bowtie antenna has reflection coefficient of -23.218 dB, bandwidth of 390 MHz, and VSWR of 1.29.

Both antennas have fulfilled the required antenna criteria, which are reflection coefficient of less than or equal to -10 dB, bandwidth of about 300 MHz, and VSWR of less than or equal to 2. In addition to that, both new modified bowtie antennas also have lower reflection coefficients and wider bandwidth compared to the modified bowtie antennas in previous research, i.e. the antenna characteristics have been improved.

Finally, the rounded-edge and the middle-sliced modified bowtie antennas have successfully detected the PD signal in the air from a needle-plane electrode, shown by PD waveforms that occur during measurement. Additionally, (φ-q-n) pattern also shows that both antennas are able to measure PD with correct phase patterns according to the electrode as the PD source. The result also shows that the middle sliced modified bowtie antenna is more sensitive in detecting PD than the rounded edge modified bowtie antenna. The smaller gain that this antenna has compared to the rounded edge modified bowtie antenna can be compensated by adding amplifier, which will be our future works.

Toward practical application, analysis of the gain characteristic of these modified UHF bowtie antennas with and without an amplifier, as well as experimental verification of PD detection using these modified bowtie antennas in a GIS environment will also be our future works.

REFERENCES

[1] M. D. Judd, O. Farish, J. S. Pearson, and B. F. Hampton, "Dielectric windows for UHF partial discharge detection," *IEEE Trans. Dielectr. Electr. Insul.*, vol. 8, no. 6, pp. 953–958, Dec. 2001.

[2] M. Hikita, S. Ohtsuka, and S. Matsumoto, "Recent trend of the partial discharge measurement technique using the UHF electromagnetic wave detection method," *IEEJ Trans. Electr. Electron. Eng.*, vol. 2, no. 5, pp. 504–509, Sep. 2007.

[3] W. A. Putro, Sriyono, K. Nishigouchi, U. Khayam, Suwarno, M. Kozako, M. Hikita, K. Urano, and C. Min, "PD pattern of various defects measured by UHF external sensor on 66 kV GIS model," in *Proc. CMD*, Bali, Indonesia, 2012, pp. 954–957.

[4] W. A. Putro, K. Nishigouchi, U. Khayam, M. Kozako, M. Hikita, K. Urano, and C. Min, "Influence of spacer aperture size on PD-induced electromagnetic wave measured with UHF external sensor in 66 kV GIS model," in *Proc. IEEE Int. Conf. Condition Monitor. Diagnosis*, Sep. 2012, pp. 387–391.

[5] S. H. Maruyama, T. Hoshino, T. Sakakibara, T. Mizojiri, and H. Murase, "Sensitivity characteristics of various UHF sensors attached outside a GIS tank," in *Proc. CMD*, Tokyo, Japan, 2010, pp. 489–492.

[6] J. S. Pearson, B. F. Hampton, and A. G. Sellars, "A continuous UHF monitoring for gas insulated substations," *IEEE Trans. Elect. Insul.*, vol. 26, no. 3, pp. 169–478, Jun. 1991.
[7] R. Kurrer and K. Feser, "The application of ultra-high-frequency partial discharge measurements to gas-insulated substations," *IEEE Trans. Power Del.*, vol. 13, no. 3, pp. 777–782, Jul. 1998.
[8] S. M. K. Azam, M. Othman, H. A. Illias, T. A. Latef, M. T. Islam, and M. F. Ain, "Ultra-high frequency printable antennas for partial discharge diagnostics in high voltage equipment," *Alexandria Eng. J.*, vol. 64, pp. 709–729, Feb. 2023.
[9] H. Andre, P. Emeraldi, A. Hazmi, E. P. Waldi, and U. Khayam, "Long bowtie antenna for partial discharge sensor in gas-insulated substation," in *Proc. Int. Conf. High Voltage Eng. Power Syst. (ICHVEPS)*, Oct. 2017, pp. 175–178.
[10] F. Vauzia and U. K. Suwarno, "Design and implementation of double layer printed bowtie antenna as UHF sensor for partial discharge measurement," in *Proc. ICSSA*, Bandung, Indonesia, 2014, pp. 1–4.
[11] J. Muslim, A. Susilo, K. Nishigouchi, Y. Z. Arief, U. Khayam, M. Kozako, and M. Hikita, "Improvement of bowtie UHF antenna model for detecting PD in GIS," *Proc. Technol.*, vol. 11, pp. 227–234, Jan. 2013.
[12] H. Andre and U. Khayam, "Design of new shape printed bowtie antena for ultra high frequency partial discharge sensor in gas-insulated substations," in *Proc. Int. Conf. Inf. Technol. Electr. Eng. (ICITEE)*, Oct. 2013, pp. 355–359.
[13] J. Muslim, A. Susilo, K. Nishigouchi, M. Kozako, M. Hikita, Y. Z. Arief, U. Khayam, and Suwarno, "Enhanced bowtie UHF antenna for detecting partial discharge in gas insulated substation," in *Proc. 48th Int. Universities' Power Eng. Conf. (UPEC)*, Sep. 2013, pp. 1–5.
[14] A. A. Lestari, A. G. Yarovoy, and L. P. Ligthart, "An efficient ultra-wideband bow-tie antenna," in *Proc. 31st Eur. Microw. Conf.*, Sep. 2001, pp. 120–132.
[15] B. Allen, M. Dohler, E. E. Okon, W. Q. Malik, A. K. Brown, and D. J. Edwards, *Ultra-Wideband Antennas and Propagation: For Communications, Radar and Imaging*. Hoboken, NJ, USA: Wiley, 2007.
[16] Y.-L. Chen, C.-L. Ruan, and L. Peng, "A novel ultra-wideband bowtie slot antenna in wireless communication systems," *Prog. Electromagn. Res. Lett.*, vol. 1, pp. 101–108, 2008.
[17] P. Silvester, "Finite element analysis of planar microwave networks," *IEEE Trans. Microw. Theory Techn.*, vol. MTT-21, no. 2, pp. 104–108, Feb. 1973.
[18] A. Reineix and B. Jecko, "Analysis of microstrip patch antennas using finite difference time domain method," *IEEE Trans. Antennas Propag.*, vol. 37, no. 11, pp. 1361–1369, Nov. 1989.
[19] L. Li, C. Huang, Y. Zeng, and X. Jiang, "Partial discharge diagnosis on GIS based on envelope detection," *WSEAS Trans. Syst.*, vol. 7, no. 11, pp. 1238–1247, Nov. 2008.
[20] K. He, J. Chen, and Z. Zhang, "Bowtie nanoantennas with void defects," in *Proc. Photon. Global Conf. (PGC)*, Dec. 2012, pp. 1–3.
[21] A. A. Suryandi and U. Khayam, "Design of new shape of bowtie antenna with edge modification for UHF partial discharge measurement," in *Proc. 2nd IEEE Conf. Power Eng. Renew. Energy (ICPERE)*, Dec. 2014, pp. 257–261.
[22] S. Qu and C. Ruan, "Quadrate bowtie antenna with round corners," in *Proc. IEEE Int. Conf. Ultra-Wideband*, Sep. 2005, pp. 93–96.
[23] S. W. Qu and C. L. Ruan, "Effect of round corners on bowtie antennas," *Prog. Electromagn. Res.*, vol. 57, pp. 179–195, 2006.
[24] A. A. Suryandi and U. Khayam, "New designed bowtie antenna with middle sliced modification as UHF sensor for partial discharge measurement," in *Proc. Int. Conf. Smart Green Technol. Electr. Inf. Syst. (ICSGTEIS)*, Nov. 2014, pp. 98–101.

UMAR KHAYAM (Member, IEEE) received the B.Sc. and M.Sc. degrees from the Department of Electrical Engineering, Institut Teknologi Bandung, Indonesia, in 1998 and 2000, respectively, and the doctoral degree from Kyushu Institute of Technology, Japan, in 2008.

He is currently an Associate Professor with the Power Engineering Research Group, School of Electrical Engineering and Informatics, ITB He is also the Head of the Laboratory of High-Voltage and High-Current Engineering and the Doctoral Study Program of Electrical Engineering and Informatics, ITB. He has published more than 161 international conference papers and journal articles. His research interest includes high-voltage engineering, mainly on the development of diagnosis system of power apparatus based on partial discharge measurement techniques. He received the best paper award from international conferences, in 2005, 2014, 2016, 2018, and 2022.

ASEP ANDI SURYANDI was born in Indonesia, in 1986. He received the B.Sc. degree from Sekolah Tinggi Teknik PLN (STT-PLN)/School for Engineering of PLN's Foundation, in 2008, the M.Eng. degree in electrical engineering from the Bandung Institute of Technology, Indonesia, in 2015. He is currently pursuing the Ph.D. degree with The University of Manchester, U.K.

He worked as an Electrical Engineer at the Agency for the Assessment and Application of Technology, Indonesia, from 2010 to 2021. Since 2021, he has been working as a Senior Engineer with the National Research and Innovation Agency—BRIN, Indonesia. His research interests include finite element method, electromagnetic analysis, sensor and electric machine design, and condition monitoring in high-voltage apparatus and electric machines.

RACHMAWATI was born in Indonesia, in 1988. She received the B.Sc. degree in electrical engineering from the Bandung Institute of Technology (ITB), Indonesia, in 2010, the M.Eng. degree from Tohoku University, Japan, in 2013, and the doctoral degree in electrical engineering from Nagoya University, Japan, in 2022.

She was an Academician at the School of Engineering and Informatics (SEEI), ITB, from 2017 to 2019, where she has been a Research Assistant, since 2022.

Dr. Rachmawati received the Best Paper Prize from the IEEE Sendai Section, in 2013. She also received Best Presentation Awards from ISEIM, Japan, in 2020, IEE, Japan, in 2020 and 2021, and ISH, China, in 2021.